行政院國家科學委員會專題研究計畫 成果報告

利用碳奈米管製備超電容電極之研究
研究成果報告(精簡版)

計 畫 類 別 ：個別型
計 畫 編 號 ：NSC 96-2221-E-216-013-
執 行 期 間 ：96 年 08 月 01 日至 97 年 07 月 31 日
執 行 單 位 ：中華大學機械工程學系

計 畫 主 持 人：林育立

計畫參與人員：碩士班研究生-兼任助理人員：劉安鈞
碩士班研究生-兼任助理人員：潘威仁
碩士班研究生-兼任助理人員：曾偉倫
博士班研究生-兼任助理人員：黃厚升

報 告 附 件 ：出席國際會議研究心得報告及發表論文

處 理 方 式 ：本計畫可公開查詢

中 華 民 國 97 年 10 月 11 日

利用碳奈米管製備超電容電極之研究

計畫編號：NSC 96－2221－E－216－013

執行期間： 96 年 8 月 1 日至 97 年 7 月 31 日

計畫主持人：林育立

摘　要

本研究利用陰極沈積法將含水釕化物與碳奈米管沈積在鈦基材上，利用循環伏安法探討鍍層的電容特性，SEM 觀察鍍層形貌。實驗結果顯示，陰極沈積法比其它方法更能快速且有效地製作含水釕化物鍍層，且此鍍層所測得之電容量可達 590F/g。若碳奈米管再經過超音波物理性分散與界面活性劑的化學性分散作用後，則鍍層所測得之電容量可增為 718.8F/g。

關鍵字：超電容、含水釕化合物，陰極沈積法，循環伏安法、碳奈米管。

Abstract

Hydrous ruthenium oxide was deposited on Ti substrate utilizing cathodic deposition method. The electric capacity characteristics of the deposits were examined by cyclic voltammetry. The surface morphology of coatings was examined by SEM. A coating layer of hydrous ruthenium oxides with carbon nano-tube produced through cathodic deposition was found to be faster and effectively than any other methods. The measured capacitance of hydrous ruthenium oxides coating can be reached to 590F/g. However, the capactance can be increased to 718.8F/g when carbon nanotube was dispersed by using the ultrasonic vibration and surface-active agent added in the deposition bath.

Key word: supercapacitor, hydrous ruthenium oxides, cathodic deposition, cyclic voltammetric,carbon nano-tube.

1. 前言

在現今市場中，能夠提供功率平佈功能的元件以電容器最為普遍。然而，一般電容器所能提供的功率密度有限，無法適用於啟動時需高功率密度的器具。對這些電器而言，若能藉由材料的研究，開發超大容量之電容器，將可有效解決上述問題，同時提供另一種能量儲存模式。超電容除了必須兼顧輕、薄、短、小等優勢條件外。在製程上也必須尋找出新的方法，以取代製造超電容傳統繁瑣的步驟，以增進元件量化的生產速度。

超電容，或稱為電化學電容器（Ultracapacitor、Supercapacitor、Electrochemical Capacitor），是一種性能介於二次電池與傳統電容之間的電能儲存器。超電容與二次電池相比，具有更高的功率密度與更長的的充放電循環使用壽命，與傳統電容相比則具有更大的能量密度，此外還具有免維護，高可靠性的優點。且具有高瞬時功率，又不會佔據許多空間 [1]。

超電容的種類依其工作原理分為：一、電雙層，二、擬電容。電雙層超電容是利用電極與電解液之間的庫侖靜電力造成電荷分離現象進而達到儲存電能之目的。"碳–超電容"為電雙層型超電容的代表[2]。至於擬電容，不僅具備有電雙層效應，更因表面反應的電荷轉移而形成的法拉第電流，因而有比電雙層超電容大 5～10 倍的電容量。擬電容常使用的材料又可分兩大類：一、金屬氧化物；二、導電高分子薄膜 [3，4]。RuO_2 為擬電容在金屬氧化物裡的材料的典型範例。

含水釕化物 $RuO_2.xH_2O$，H^+ 離子容易在其體相中傳輸，而含水釕化物中的 Ru^{4+} 也能起作用，從而大大提升電容量。另外，再加上 *Ru* 本身有多組氧化態，可自身進行氧化還原反應 (Redox)，再加上電吸附/脫附 (Electro sorption / Desorption)的可逆反應，因此在含水釕化合物超電容中水和無定型 RuO_2 是很好的活性物質型態，其電荷的儲存遠大於傳統的電容器與電雙層電容器。化學式(1)可以用來說明 RuO_2 的氧化還原機構 [3]：

$$RuO_{a-\delta}(OH)_{b+\delta} \Leftrightarrow RuO_a(OH)_b + \delta H^+ + \delta e^- \text{----------（1）}$$

其中，$RuO_{a-\delta}(OH)_{b+\delta}$ 為低氧化態的活性釕，

$RuO_a(OH)_b$ 為高氧化態的活性釕。

此外，碳奈米管有著高比表面積以及高導電性著稱，而碳奈米管本身亦可以提供電雙層電容的效應。所以本次實驗就利用水合釕氧化物一同混合碳奈米管，取其各自所長，發展出更好的電容電極。

2. 金屬化合物電極的製備方法

文獻中常見的金屬氧化物電極製備方法有下列幾種：熱分解法（Thermal Decomposition）、溶膠-凝膠法（Sol-Gel Process）、循環伏安沈積法（Cyclic Voltammetric Deposition）、陽極氧化法

（Anodizing）、陰極沈積法（Cathodic Deposition）、化學氣相沈積（Chemical Vapor Deposition）、濺鍍法（Sputtering）和蒸鍍法（Vaporization Deposition）等方式，不同的方法可以得到不同性質的氧化物電極 [5]。

本研究選擇陰極沈積法來製備釕氧化物。由於陰極沈積法的製程步驟較為容易控制，可以降低所得試片的誤差值，同時也可藉由電位/電流的改變來控制鍍層的結構與性質。

3. 實驗方法與步驟

3.1基材前處理

選用 99.99%的鈦塊，先用丙酮去脂，再用重量百分濃度 5%的氫氟酸（HF）水溶液中進行第一階段的粗腐蝕，5 分鐘。再將粗蝕後的鈦基材置於體積百分濃度 50%的鹽酸（HCl，Merck）中，加溫至 90℃且均勻攪拌維持 15 分鐘，進行第二階段的細腐蝕。此便在鈦金屬表面獲得更多，更緻密的孔洞，進而使鍍層能在基材表面，具有更多的接觸面積，產生更強的附著力。

3.2 釕化物陰極沈積

將測重後的鈦基材接於電源供應器之陰極，以白金板作為相對陽極，裝置圖如圖 1 所示，電極置入含 $RuCl_3$ 的酸性鍍浴中，施以固定的電流通電 1～2 小時，依照所需調整實驗條件。

運用恆電位儀，以循環伏安掃瞄法來檢測所得電極之電容量。測試裝置如圖 2 所示，為典型三極式電化學分析槽。參考電極（Reference Electrode，R.E）選用甘汞電極 Hg/Hg_2Cl_2（Saturated Calomel Electrode，S.C.E），對應電極（Counter Electrode，C.E）為白金板，工作電極（Working Electrode，W.E）則為有鍍釕化物鍍層的鈦金屬，電解質為 0.5M 的硫酸水溶液，電位掃瞄範圍在 0V～1V 之間，掃瞄速度 25mV/sec 。完成後將基材低溫(40℃)吹乾，避免溫度過高而使鍍層發生變化，也避免因為含有水分而測重失準，再用精密電子微量天平測電鍍後的重量，並分別計算單位重量與單位面積之電容量。

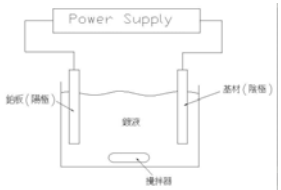

圖 1、電鍍過程示意圖

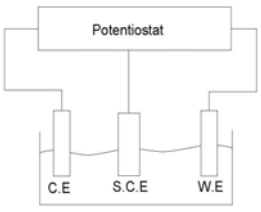

圖 2、C.V 掃瞄示意圖

3.3 釕化物的沈積與電容量計算

在一定時間內，藉由固定電流完成超電容的沈積製作。在沈積的過程中，可以清楚的觀察到釕化合物會漸漸附著於基材上（此時基材會從原本的銀灰色轉變成黑色的表面如圖 3 所示），代表在其表面有鍍上一層物質。接著清洗乾淨後，便可以進行釕化合物的電容特性測量與觀測。

方程式(2)定義，電容為在某一個電壓範圍內，所能儲存的電量(其中 C 代表電容，單位法拉、Q 代表電量，單位為庫倫，而 V 則是施加的電壓，單位為伏特)。

$$C = \frac{Q}{V} \text{ ---------- (2)}$$

然而實際上，實際釕化合物電容器，在掃描過程中，電極上的釕化合物進行著氧化還原反應，因而會得到是一種不規則逆 S 形的封閉曲線，如圖 4 所示。將曲線下面積積分就可得到電量，如此便可以計算電容大小。若對方程式(2)的分子與分母分別對時間作微分，則可延伸出電流對掃描速度的關係式(3)，取圖 4 中較平緩之電流部分為 i 值除以其掃描速度，此時所得的 C 即是電容量。方程式(2)對 t 做積分可得:

$$C = \frac{dQ/dt}{dV/dt} = \frac{i}{\upsilon} \quad (i \text{ 為電流}),(\upsilon \text{ 為掃瞄速度}) \text{--(3)}$$


圖 3、釕化合物附著於基材上

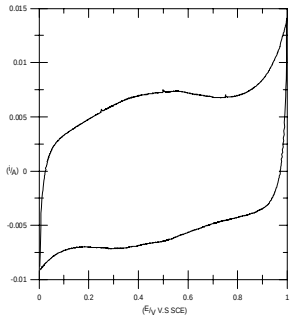

圖 4、實際狀態之 CV 圖

4. 結果與討論

4.1 添加分散後碳奈米管的電極表面型態

圖 5-圖 8 分別是添加各種不同比例的分散的碳奈米管，其添加的比例分別為 0.1%，0.05%，0.025%及 0.0125%等四種。而在每一種的濃度之中，我們又以沉積時間做為另一個實驗參數。在圖 5(a),(b),(c),(d)及(e)分別為鍍液添加超音波分散過

後 0.1wt%碳奈米管沈積時間 5 分鐘， 沈積時間 10 分鐘，沈積時間 15 分鐘，沈積時間 30 分鐘及沈積時間 60 分鐘後之鍍層結構。從圖中可觀察出鍍層之厚度隨著沉積時間的增長，厚度有逐漸增加的趨勢。圖 6-8 (a),(b),(c),(d)及(e)分別為鍍液超音波分散過後添加 0.1wt%,0.05%，0.025%及 0.0125%碳奈米管且沈積時間分別為沈積 5 分鐘， 沈積時間 10 分鐘，沈積時間 15 分鐘，沈積時間 30 分鐘及沈積時間 60 分鐘後之鍍層結構。從圖 5-圖 8 中，沉積 5 分鐘的試片明顯的發現碳奈米管的所佔量都比較少。不過碳奈米管因為做過分散處理的關係，碳奈米管鍍層分散的確是比較均勻。不過就分散的角度分析，應還有進步的空間。

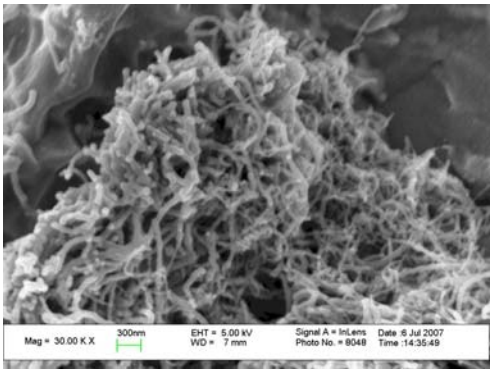

(a)

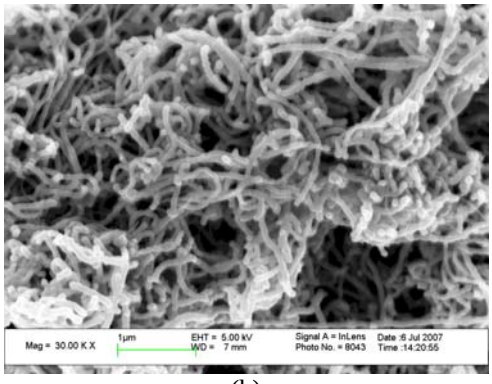

(b)

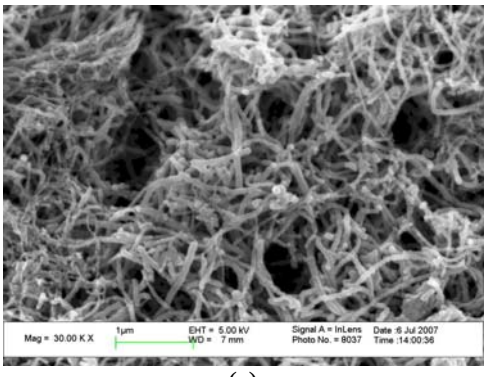

(c)

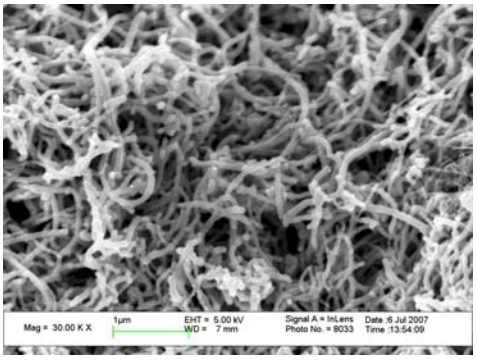

(d)

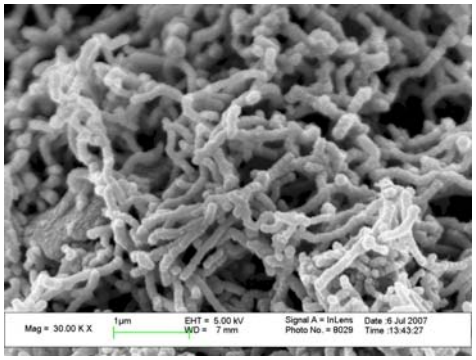

(e)

圖 5 鍍液添加超音波分散過後 0.1wt%碳奈米管(a)沈積時間 5 分鐘， (b)沈積時間 10 分鐘，(c)沈積時間 15 分鐘，(d)沈積時間 30 分鐘及(e)沈積時間 60 分鐘後之鍍層結構

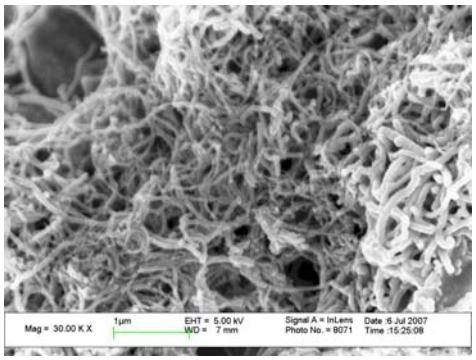

(a)

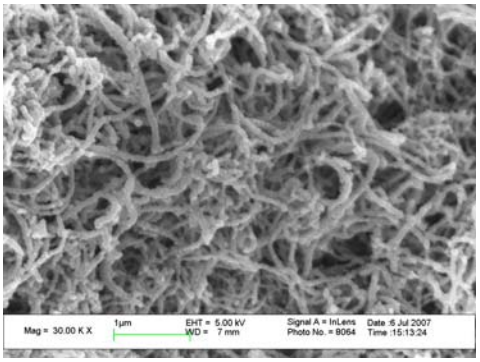

(b)

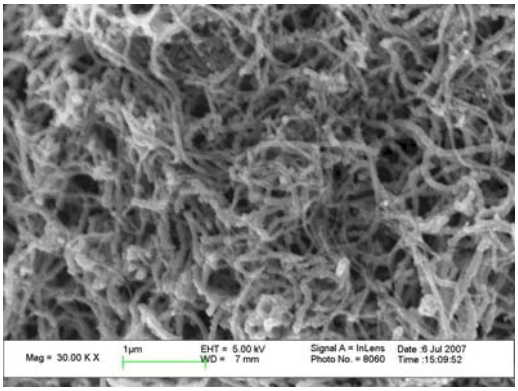

(c)

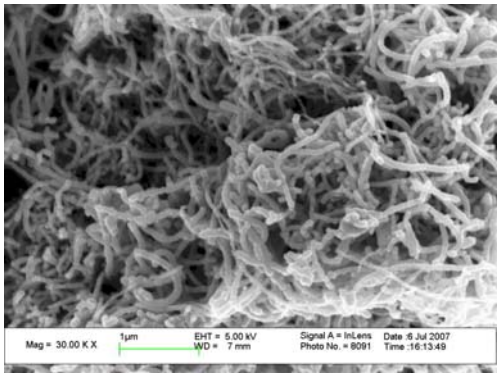

(a)

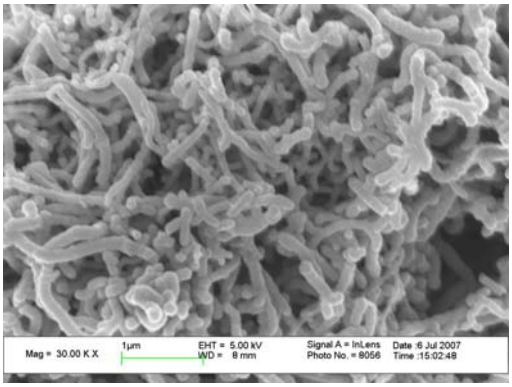

(d)

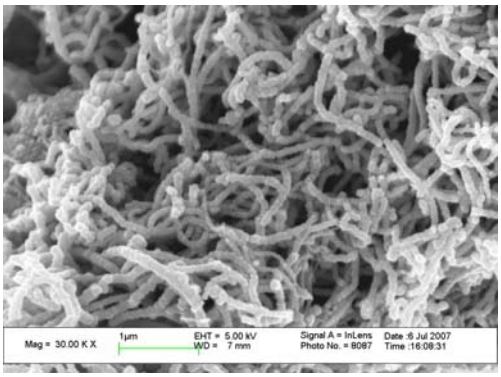

(b)

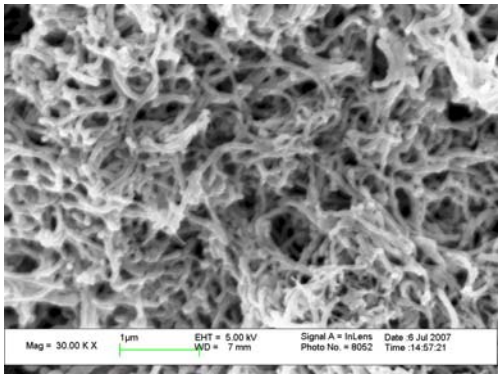

(e)

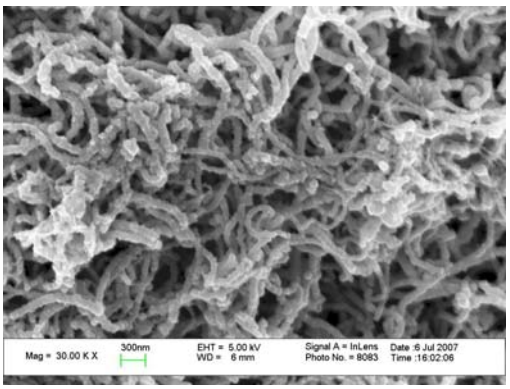

(c)

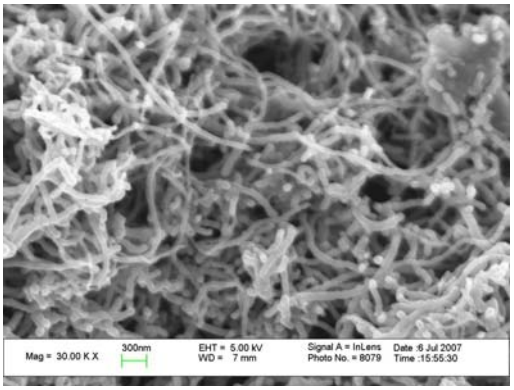

(d)

圖 6 鍍液添加超音波分散過後 0.05wt%碳奈米管(a)沈積時間 5 分鐘， (b)沈積時間 10 分鐘，(c)沈積時間 15 分鐘，(d)沈積時間 30 分鐘及(e)沈積時間 60 分鐘後之鍍層結構

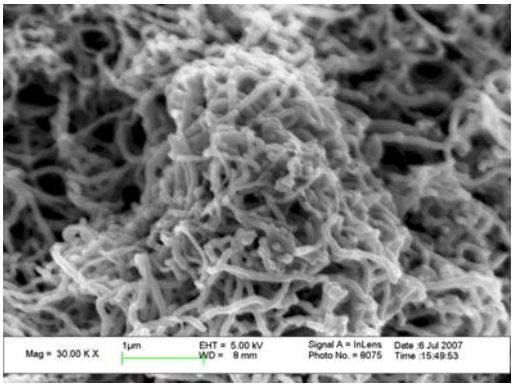

(e)

圖 7 鍍液添加超音波分散過後 0.025wt%碳奈米管 (a) 沈積時間 5 分鐘， (b)沈積時間 10 分鐘，(c)沈積時間 15 分鐘，(d)沈積時間 30 分鐘及(e)沈積時間 60 分鐘後之鍍層結構

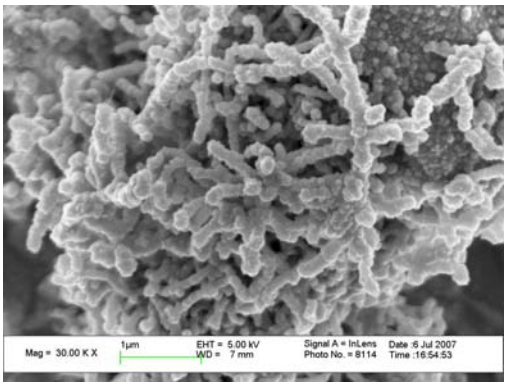

(a)

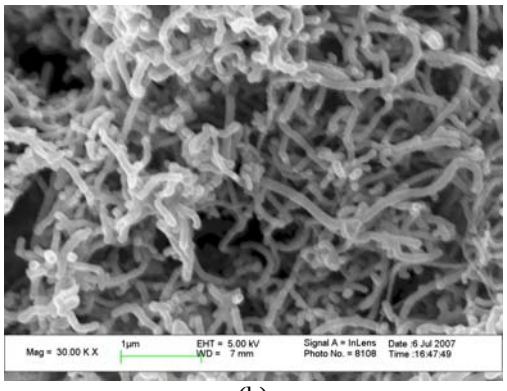

(b)

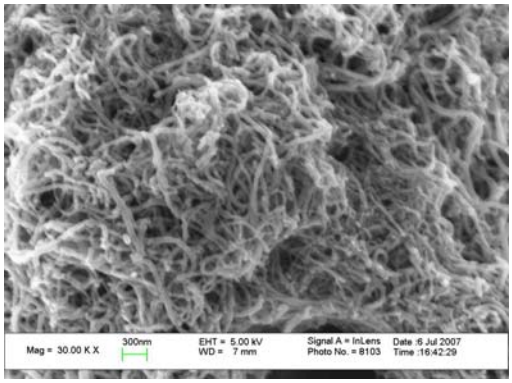

(c)

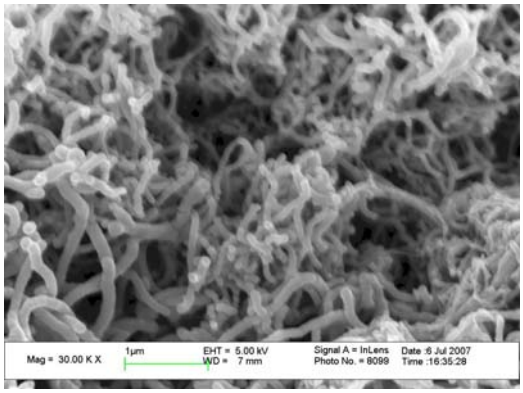

(d)

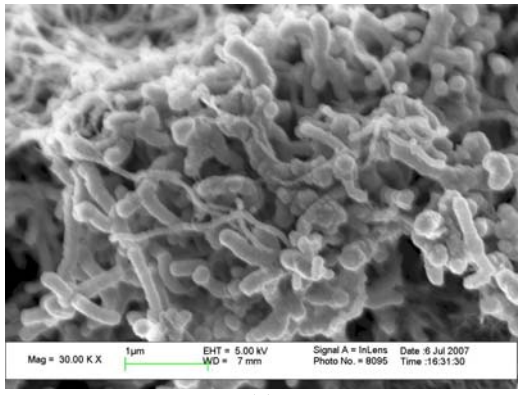

(e)

圖 8 鍍液添加超音波分散過後 0.0125wt%碳奈米管 (a) 沈積時間 5 分鐘， (b)沈積時間 10 分鐘，(c)沈積時間 15 分鐘，(d)沈積時間 30 分鐘及(e)沈積時間 60 分鐘後之鍍層結構

4.2 電容量特性探討

4.2.1 以沈積時間作為變數探討電容量特性

圖 9 為添加 0.1wt%超音波分散過後碳奈米管在不同沈積時間所得電容特性曲線圖，圖 10 為添加 0.05wt%超音波分散過後碳奈米管在不同沈積時間所得電容特性曲線圖，圖 11 為添加 0.025wt%超音波分散過後碳奈米管在不同沈積時間所得電容特性曲線圖及圖 12 為添加 0.0125wt%超音波分散

過後碳奈米管在不同沈積時間所得電容特性曲線圖。從圖形的面積即可約略觀察出電容量之大小，一般而言，在相同之添加量之下，其電容量隨著沈積時間的增加而有增加的趨勢。

圖 13 為添加分散後碳奈米管不同濃度之電容量趨勢圖。在圖 13 中，以添加 0.05wt%的分散碳奈米管之表現最為搶眼，從圖中可明顯觀察出沈積時間為 60 分鐘所測得之電容量為所有條件中之最高者，電容量為 718.8F/g。

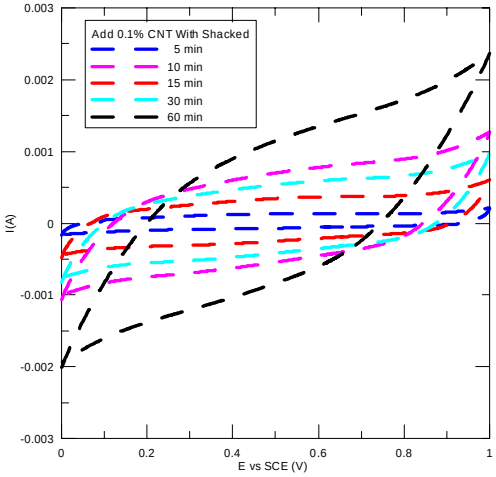

圖 9 添加 0.1wt%超音波分散過後碳奈米管在不同沈積時間所得電容特性曲線圖

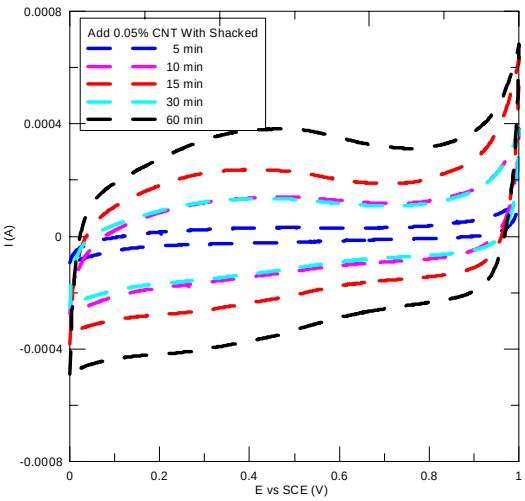

圖 10 添加 0.05wt%超音波分散過後碳奈米管在不同沈積時間所得電容特性曲線圖

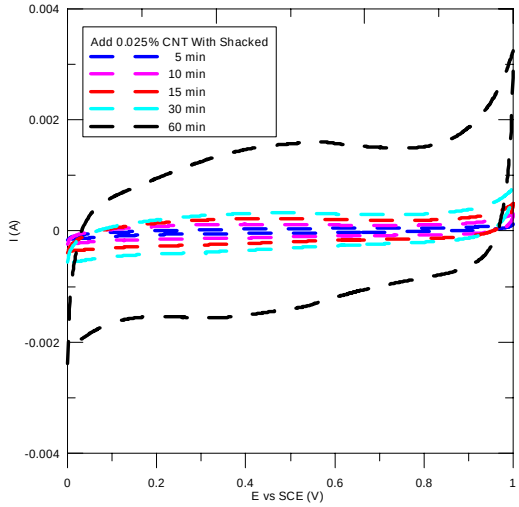

圖 11 添加 0.025wt%超音波分散過後碳奈米管不同沈積時間所得電容特性曲線圖

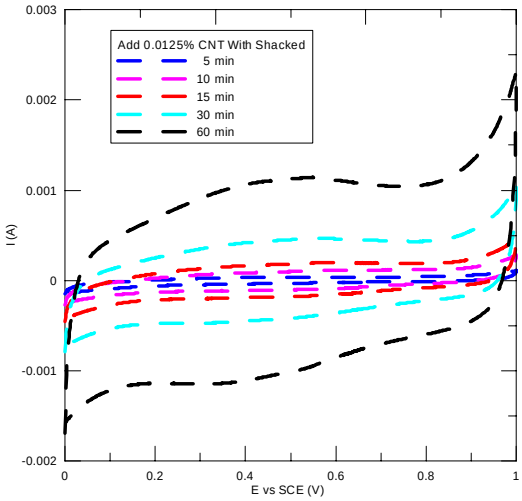

圖 12 添加 0.0125wt%超音波分散過後碳奈米管不同沈積時間所得電容特性曲線圖

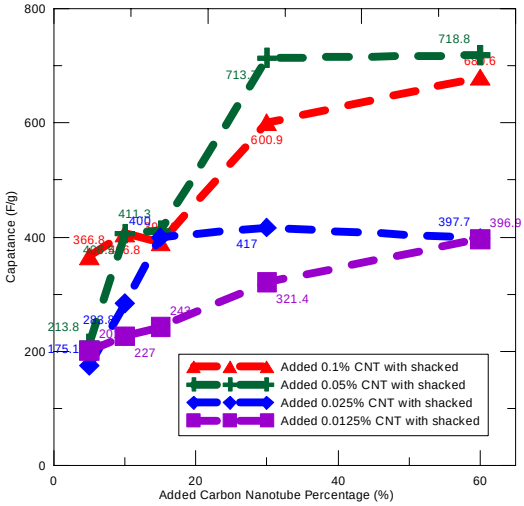

圖 13 不同添加分散碳奈米管濃度之電容量趨勢圖，紅線為添加 0.1%、綠線為添加 0.05%、藍線為添加 0.025%以及紫線為添加 0.0125%。

4.2.1 以添加分散的碳奈米管濃度為變數探討電容量特性

圖 14-圖 18 所呈現的就是在固定沈積時間參數後，添加不同碳奈米管濃度的循環伏安曲線圖。圖 14 為添加不同碳奈米管濃度的分散碳奈米管在沈積 5 分鐘所得之電容特性曲線圖，圖 15 為添加不同碳奈米管濃度的分散碳奈米管沈積 10 分鐘所得之電容特性曲線圖，圖 16 為添加不同碳奈米管濃度的分散碳奈米管沈積 15 分鐘所得之電容特性曲線圖，圖 17 為添加不同碳奈米管濃度的分散碳奈米管沈積 30 分鐘所得之電容特性曲線圖，而圖 18 為添加不同碳奈米管濃度的分散碳奈米管沈積 60 分鐘所得之電容特性曲線圖。從圖形的面積即可約略觀察出電容量之大小，一般而言，在固定沈積時間之下，其電容量隨著添加碳奈米管濃度的增加而有增加的趨勢。

圖 19 為固定分散碳奈米管濃度，改變沈積時間之電容量趨勢圖。在圖 19 中，在沈積時間為 60 分鐘與 30 分鐘的表現最好， 惟沈積時間 30 分鐘與沈積時間 60 分鐘的表現相比，其所測得之電容量並不會相距太多。

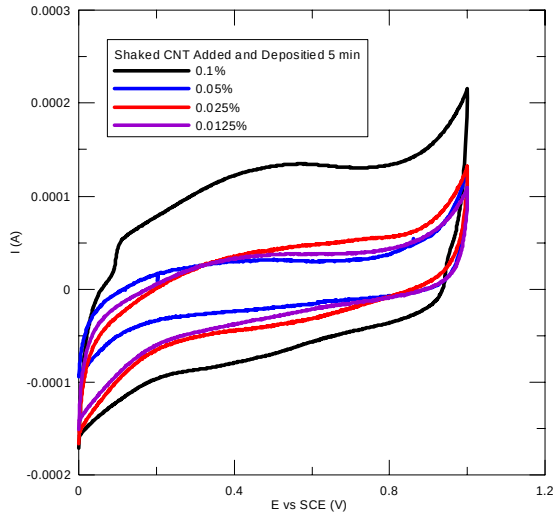

圖 14 添加不同濃度的分散碳奈米管在沈積 5 分鐘所得之電容特性曲線圖

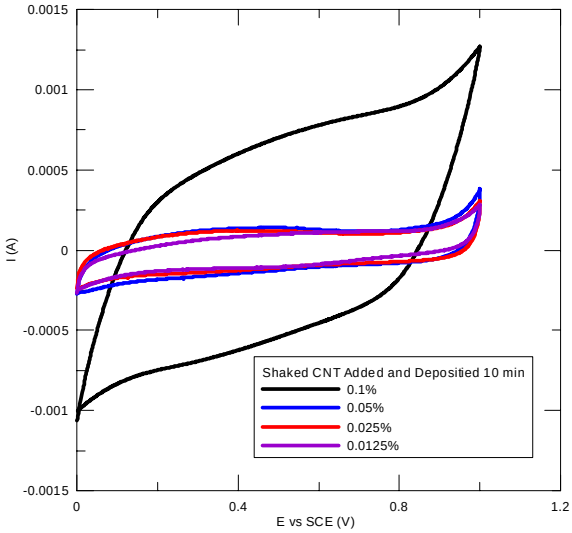

圖 15 添加不同濃度的分散碳奈米管在沈積 10 分鐘所得之電容特性曲線圖

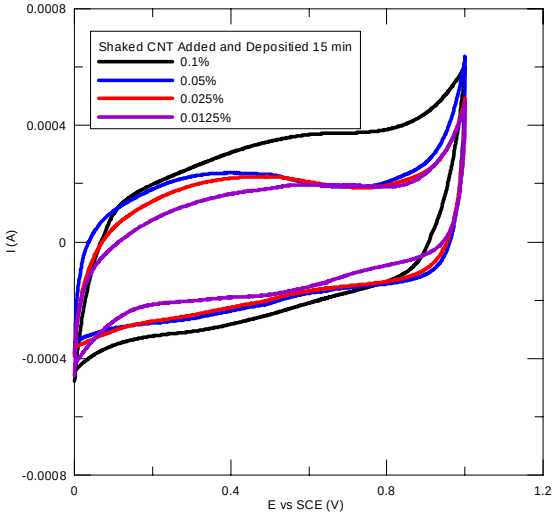

圖 16 添加不同濃度的分散碳奈米管在沈積 15 分鐘所得之電容特性曲線圖

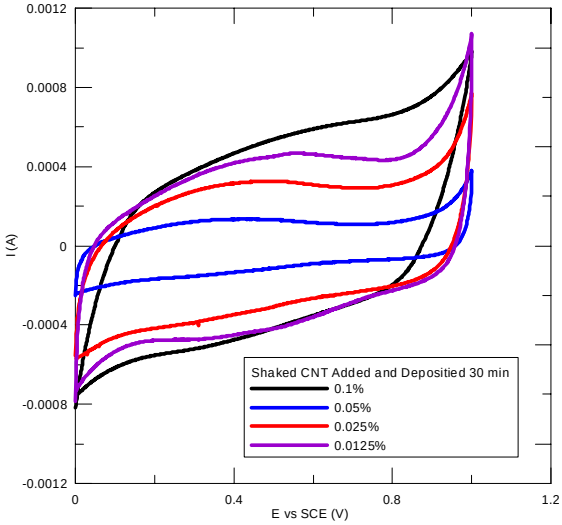

圖 17 添加不同濃度的分散碳奈米管在沈積 30 分鐘所得之電容特性曲線圖

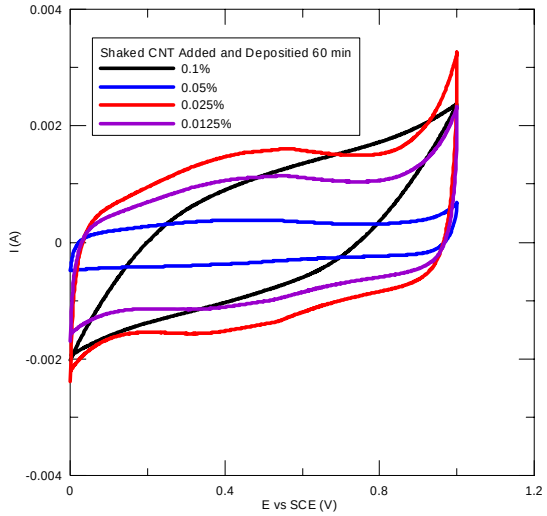

圖 18 添加不同濃度的分散碳奈米管在沈積 60 分鐘所得之電容特性曲線圖

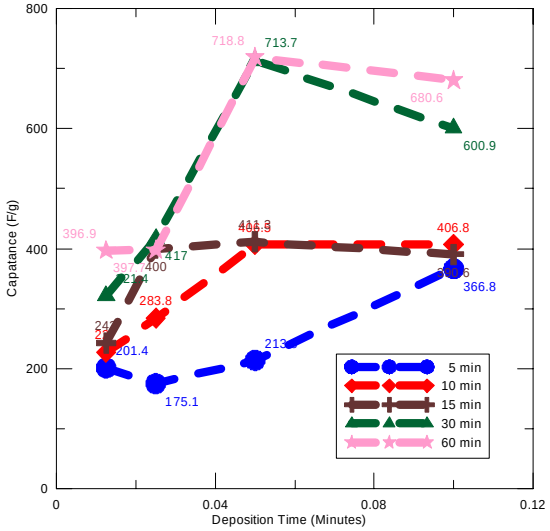

圖 19 固定分散碳奈米管濃度，變數為沈積時間之綜合電容量趨勢圖，藍線沈積 5 分鐘、紅線沈積 10 分鐘、棕線沈積 15 分鐘、綠線沈積 30 分鐘以及粉紅線沈積 60 分鐘。

5 結論

本此實驗我們使用了物理及化學方式來分散碳奈米管，藉此提升碳奈米管的使用效率，以及減少碳奈米管的使用量。首先添加界面活性劑於添加碳奈米管的溶液之中，然後再利用高功率超音波的震盪將碳奈米管分散。此時界面活性劑會附著於分散的碳奈米管表面，而使其不易產生團聚現象。

實驗結果顯示，添加分散的碳奈米管重量百分濃度 0.05%，沈積時間為 60 分鐘所測得之電容量最大為 718.8F/g。不過我們也發現本此實驗最適當的碳奈米管濃度並不是 0.1wt%而是 0.05wt%。由於分散的作用使得只需要微量的碳奈米管就可以發揮不錯的效應。

6.感謝

本項研究感謝國科會(NSC 96-2221-E 216-013)提供資助才得以完成。

7.參考文獻

1. 超高容量電容及電池混合店員模組之應用，陳元杰，廖秋峰。工業材料雜誌 178 期 p100~106，90 年 10 月。
2. Electrochemical Capacitors Utilizing Low Surface Area Carbon Fiber. Stephen M. Lipka. *IEEE AES Systems Magazine, July 1997.*
3. 釕氧化物超高電容材料特性簡介，黃孟娟，張榮錡，工業材料雜誌 182 期 p120~128，91 年 2 月。
4. The Specific Influence of Hydrogen Ions on Poly (Pyrrole) Potentionmetry. Agata Michalska, Krzysztof Maksymiuk. *Electrochimical Acta 44 (1999) 2125-2129.*
5. 超高電容器製程技術簡介，高志勇，陳耿陽，吳富其，江萬爵，賴志坤。工業材料雜誌 166 期 p113~119，89 年 10 月。
6. 含水氧化錳電極之製備與擬電容特性研究，張仍奎，蔡文達 *(NSC-90-2216-E-006-070)*，2002 年材料年會 PE-17。
7. H.-S. Hwang, Yuli Lin, Composite Supercapacitor of Hydrous Ruthenium Oxides and Carbon NanotubeEee, Chung Hua Journal of Science and Engineering, Vol. 6, No. 2, pp. 41-44 (2008)
8. Yuli Lin, H.-S Hwang and Wen-Jin Lee, Composite Supercapacitor of Hydrous Ruthenium Oxides and Carbon Nanotube Coatings on Ti Substrate by Cathodic Deposition Method, Microscopy and Microanalysis 13(Suppl 2),994-995 2007
9. Yuli Lin and H.-S Hwang, Effect of Graphite Concentration on the Capacitance of Composite Supercapacitor of Hydrous Ruthenium Oxides Coatings by Cathodic Deposition Method, Microscopy and Microanalysis 13(Suppl 2),996-997 2007.
10. H.-S. Hwang and Yuli Lin,Hydrous ruthenium oxide coating on Ti and carbon nanotube substrate for the electrode of supercapacitor, International Conference, Thin Film 2008, Singapore.

8.自評

本計畫執行成果豐碩，不僅達成原有之目標且有超前，本計畫之成果也已投稿國內期刊論文一篇及國外一篇及參加研討會發表三篇論文。

行政院國家科學委員會補助國內專家學者出席國際學術會議報告

計畫編號	NSC 96-2221-E-216-013
計畫名稱	利用碳奈米管製備超電容電極之研究
出國人員姓名 服務機關及職稱	林育立 中華大學機械工程學系教授
會議時間 地點	自 97 年 7 月 13 日至 97 年 7 月 16 日 新加坡
會議名稱	第四屆薄膜與表面鍍層國際研討會 The 4th International Conference on Technological Advances of Thin Films & Surface Coatings
發表論文題目	1. **Hydrous ruthenium oxide coating on Ti and carbon nanotube substrate for the electrode of Supercapacitor** 2. **High reflectance metallic thin films of reference mirror layers on sapphire substrate for LED devices**

一、參加會議經過

本次會議(第四屆薄膜與表面鍍層國際研討會)於九十七年七月十三日至七月十六日共計四日，筆者於七月十三日搭乘長榮航空班機於中午十二時抵達新加坡樟宜國際機場，隨即搭車至市中心文華酒店，稍作休息後即搭乘地下鐵赴本次會議之場所:新加坡管理大學(SMU Admin.)， 今天因尚無演講活動因此辦完一切手續後就返回飯店。本次會議空前浩大，有來自全世界超過三十個國家共發表超過七百篇之論文，其中有兩百多篇為口頭講演及四百多篇之論文展示。此次會議也與另一研討會”NanoMan: The 1st International Conference on Nanomanufacturing”共同舉辦，垓研討會共有接近兩百篇論文。筆者此次共發表兩篇文章，其中一篇為口頭報告另外一篇則為論文海報展示。第二天一大早就到會場，因昨晚事先已擬妥今天要聽的場次，因此早上就聽了幾場有興趣的研究報告，尤其是會議一開始網網邀請重量級之演講者，這種演講更是筆者一定不會放過的。另外早上十點十五分在口頭報告的中場休息時間也穿插論文海報展示的活動。與一般上台口頭報告不同，海報可以放的東西比較多且展示時間也較長，加上作者可以在旁即時解釋及討論論文內容，而且同一時間有幾十甚至上百篇論文同時展示，因此其重要性並不輸於比口頭報告。筆者對於材料方面尤其是鍍層方面較有興趣，因此選擇的聽講題目大都在這個領域，筆者也發現雖然此次會議奈米材料的題材還是受到重視，不過奈米材料的發展好像也達到一定的瓶頸，最近此領域熱門的程度有下降的趨勢，隨著全球能源的愈來愈缺乏，最近對於能源材料方面的研究有漸趨熱絡的趨勢，這也可給我們作為未來研究的參考。筆者的論文為星期一上午一點十五分的海報發表，及星期下午三點五十分之口頭報告，因筆者所研究不僅利用顯微鏡觀察材料之性質更結合奈米材料及能源方面的應用，因此吸引不少來自世界各國研究者的目光與興趣，會議最後在十六日下午六點是四十五分最後一場報告後劃下句點。因本次會議結束時間時間較晚因此只能搭乘十七日之班機回國。

二、與會心得

此次會議有超過來自全世界三十多個國家一千多名學者專家與會，從會議的流程可發現主辦單位在各項安排都十分注重，可謂是成功的一次大型國際研討會。本次會議也有一些小缺點，會議之宣導並不是十分理想，因此在會議中心外之街道並無會議舉行之資訊，也有可能是新加坡政府規定。另外會議安排之地點也不太理想，並不是大型之會展中心，只利用管理大學之行政大樓來作為會議中心，這與號稱有八百餘篇參予之研討會好像不太符合。再研究主題方面雖然此次會議奈米材料的題材還是受到重視，不過奈米材料的發展好像也達到一定的瓶頸，最近此領域熱門的程度有下降的趨勢，隨著全球能源的愈來愈缺乏，最近對於能源材料方面的研究有漸趨熱絡的趨勢，這也可給我們作為未來研究的參考。

三、攜回資料名稱及內容

1. Proceeding of The 4th International Conference on Technological Advances of Thin Films & Surface Coatings
2. Disk of The 4th International Conference on Technological Advances of Thin Films & Surface Coatings

四、論文

High reflectance metallic thin films of reference mirror layers on sapphire substrate for LED devices

Cheng-Yi Hsu[1,2], Mei-Lin Lin[1] and Yuli Lin[1,*]

[1]Department of Mechanical Engineering, Chung Hua University,
No.707, Sec.2, Wu-Fu Rd., Hsinchu 300, Taiwan R.O.C.

[2]Epistar Corporation, No.10 Li-hsin Rd., Science-bases Industrial Park,
Hsinchu , Taiwan 300,R.O.C.

[*]e-mail: yulilin@chu.edu.tw, TEL:886-3-5186494, FAX: 886-3-5186521

Keywords: Coatings, reflectance, thin films

Abstract. The effect of high reflectance metallic thin films of reference mirror layers is investigated using three different thin film structures on sapphire substrate: the sapphire/Ti/Ag/AuSn, sapphire/Cr/Ag/AuSn, and sapphire/Al_2O_3/Ag/AuSn structures. Various coating thickness was deposited on sapphire substrate. The experimental results indicate that the Ti and Cr buffer layer are not very effective on the enhancement of reflectance on the Ag layer. Results show that the reflectance properties of the mirror layer can be improved significantly by using Al_2O_3/Ag coating. In a buffer layer solution, the reflectance of reference mirror layer can have about 200% of improvement with the Al_2O_3 buffer layer comparing to that using Ti and Cr as the buffer layer.

1. Introduction

The silver (Ag) metal has been used widely as a reference mirror for the optospectrum meter because of its excellent optical film characteristics; it has a very high reflectance and low

transmittance on glass substrate [1]. For optospectrum meter measurements, a film type of Ag layer is preferred because it is simple in structure and durable for most mirrors. The required durability of this mirror is achieved by forming a thick Ag layer on the surface of glass [2–4]. For microscopic applications, a thin film type of Ag reference mirror layers is preferred because the well-developed technologies of semiconductor processes can be applied to fabricate a miniaturized LED (light emitting diode). Usually, the thin film of Ag reference mirror layers is fabricated on top of a Ti layer, which is formed by oxidizing the glass substrate. Much effort has been given to find a structure that is suitable for fabrication of a durable, stable, and reproducible thin film of Ag reference mirror layers. Among them, Lung-Chien Chen [5] reported the most impressive achievement of durability in a sapphire substrate solution. They used multilayers of SiO_2/TiO_2 Bragg reflector to achieve the long durability. However, the structure of SiO_2 /TiO_2 Bragg reflector with 400-700nm of thickness is more dielectric layer. On sapphire substrate, the best mirror material will be the Ag metal which not only have high reflectance for a large spectral range but also can prevent dissolution of Ag and Al_2O_3 in a solution of high adhesion. Therefore, a silver layer was intercalated between the buffer layers and the passivation layer. One problem associated with using Ag reference mirror layer with a buffer layer is that the buffer layer needs good adhesion to both sapphire substrate and Ag layer. Another problem is that the Ag layer is easy affected on process temperature. This is the reason that passivation layer is needed. When the thickness of sapphire substrate is decreased to 90 μm by grind and polish, the backside surface of sapphire substrate is roughening. Therefore, the effect of reflectance and transmittance of Ti and Cr and

Al_2O_3 buffer layers on the physical and optical properties of the thin film Ag reference mirror layer is needed to investigate. In this study, we design three thin film reference mirror layers structures: (a) Sapphire/Ti/Ag/AuSn, (b) Sapphire/Cr/Ag/AuSn and (c) Sapphire/Al_2O_3/Ag/AuSn structures for investigating the output stability and insensitivity of these reference mirror structures.

2. Experimental Procedure

An environmentally stable silver material having very high reflection values over a large spectral range is potentially utilized on sapphire substrate for LED applications. In this study, we designed three coating layers on sapphire substrate: sapphire/Ti/Ag/AuSn, sapphire/Cr/Ag/AuSn, and sapphire/Al_2O_3/Ag/AuSn. The first layer is coated as a buffer layer using materials of Ti, Cr and Al_2O_3 using e-gun deposition with the deposition rate of approximately 0.2nm/sec. for 150 and 300 seconds. The second layer is the mirror layer using material of Ag using with the deposition rate of approximately 0.5nm/sec. for 200, 1000 and 2000 seconds. The third layer is coated as the passivation layer using material of AuSn with the deposition rate of approximately 0.5nm/sec. for 6000 seconds. The optical properties of our reference mirror layer structures were measured by Hitachi U-4100 optospectrum meter. The microstructure of the reference mirror structures was observed by scanning electron microscopy (SEM). Adhesion of reference mirror structures was also measured by lap shear method.

3. Results and discussion

3.1 Microstructure and adhesion of designed reference mirror structures

Fig. 2. shows the represented microstructure of sapphire/Ti/Ag/AuSn, sapphire/Cr/Ag/AuSn, and sapphire /Al_2O_3/Ag/AuSn. Since the thickness of the first buffer layer is very thin, the microstructure is hard to investigate. The second coated layer is the Ag reference mirror layer with the thickness of about 100nm, 450nm and 900nm corresponding to sapphire/Ti/Ag/AuSn, sapphire/Cr/Ag/AuSn, and sapphire/Al_2O_3/Ag/AuSn structures, respectively. The thickness of Ag layer is a litter thinner than it was set on E-gun deposition processes. The third layer is the AuSn passivation layer with the thickness of about 3000nm. For the adhesion test, it was found that the specimen of Sapphire/Cr/Ag/AuSn structure has the best adhesion among all the specimens. The maximum adhesion strength can be reached to about 50MPa. The fracture was observed at the interface between sapphire and Ag coating layers, indicating the adhesion of sapphire/Cr interface was poor. The maximum adhesion strength was measured about 30MPa on sapphire/Ti/Ag/AuSn structure. The fracture was observed at the interface between sapphire and Ag coating layers on this specimen. On the other hand, the measured adhesion strength of sapphire/Al_2O_3/Ag/AuSn can be reached to about 11MPA. The fracture was observed at the interface between Al_2O_3 and Ag coating layers, indicating the adhesion of sapphire/Al_2O_3 had better adhesion than Al_2O_3/Ag interface.

3.2. Optical properties of designed reference mirror structures

The results of the reflectance and transmittance measurement for sapphire/Ti/Ag/AuSn, sapphire/Cr/Ag/AuSn, and sapphire/Al_2O_3/Ag/AuSn structures were shown in Table 2. These reflectance data had measured based on Al mirror after calibration on Hitachi U-4100 optospectrum

meter. On the other hand, the transmittance data had measured based on air after calibration on Hitachi U-4100 optospectrum meter. The results demonstrate that low reflectance and low transmittance on both single Ti, Cr coated layer on sapphire substrate. The measured value of reflectance is about 14% to 25% on wavelength 460nm. The Al_2O_3 coated layer on sapphire shows low reflectance as well (about 10% on wavelength 460nm). Although Ag single layer coated on sapphire shows better reflectance (about 47% to 52% on wavelength 460nm), the Ag coating layer was found easily peeled off indicating that adhesion between Ag and sapphire was poor. On multilayered structures, it can be found that low reflectance and no transmittance on sapphire/Ti/Ag /AuSn structure with various thickness of coating material. The measured value of reflectance is about 18% to 22% on wavelength 460nm. The value of transmittance is about 0% on wavelength 300 to 1600nm. On sapphire/Cr/Ag/AuSn structure, similar results can be investigated. The measured value of reflectance is about 20% to 27% on wavelength 460nm. The value of transmittance is about 0% on wavelength 300nm to 1600nm. On sapphire/Al_2O_3/Ag/AuSn structure, the value of reflectance is about 41% to 48% on wavelength 460nm and the value of transmittance is about 0% on wavelength 300nm to 1600nm. Among those structures, it was found that sapphire/Al_2O_3/Ag/AuSn structure has the best reflectance. The designed reflectance of reference mirror structure can have about 200% of improvement with the Al_2O_3 buffer layer comparing to that using Ti and Cr as the buffer layer. Fig.3 shows the reflectance profiles for the (a) sapphire/Ti/Ag/AuSn, (b) sapphire/Cr/Ag/AuSn, and (c) sapphire/Al_2O_3/Ag/AuSn structures with specimen symbols defined in Table 2.

4. Summary

1. Single layer using Ag metal was found having the best reflectance than other material on sapphire backside. The reflectance is increased with increasing the thickness of Ag coating layer. However, the adhesion of Ag single layer was found easily peeled off from the sapphire substrate.
2. On multilayer structures, it was found that the structure of sapphire/Al_2O_3/Ag/AuSn structure has the best reflectance than sapphire/Ti/Ag/AuSn and sapphire/Cr/Ag/AuSn structures. The reflectance of designed sapphire/Al_2O_3/Ag/AuSn structure can have about 200% of improvement comparing to other two structures.

5. Acknowledgements

This research was partially supported by National Science Council under contract NSC96-2221-E-216-013, Chung Hua University under contract CHU96-2221-E216-013. The measurement of optical properties in Epistar Corporation was also acknowledged.

6. References

1. G. Hass, Applied Optics and Optical Engineering**,** Vol. III (R.Kingslake , ed.), Academic, New York, chap.8, 309-330 (1965).
2. L-C. Chen and H-C. Feng, R phys. stat. sol. (a) 202, No.14, 2836–2839 (2005).
3. Y. Xi, X. Li, J. K. Kim, F. Mont, Th. Gessmann, H. Luo, and E. F. Schubert, J. Vac. Sci. Technol. A, Vol. 24, No. 4, 1627-1630 (2006).

4. T. Ive, O. Brandt, H. Kostial, T. Hesjedal, M. Ramsteiner, and H.P. Klaus, Appl. Phys. Lett.,Vol.85, No.11, 1970-1972 (1970).

5. H.R. Kim, Y.D. Kim, K.I. Kim, J.H. Shim, H. Nam, B.K. Kang, Sensors and Actuators B 97(2), 348–354 (2004).

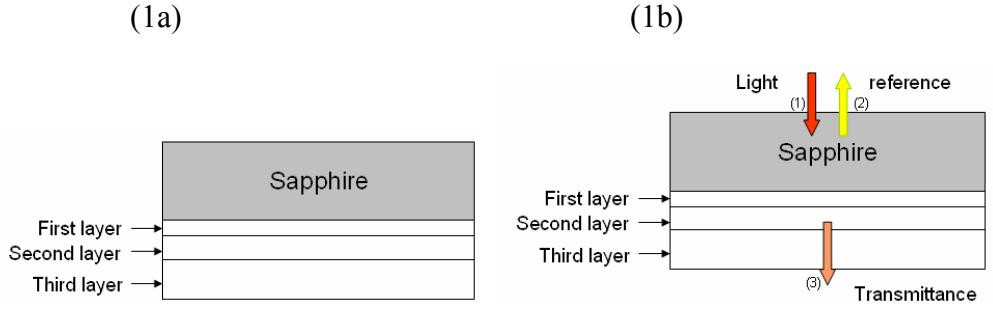

Fig. 1. A schematic diagram of the designed reference mirror structures: (a) three layers of coating at the backside of sapphire substrate and (b) the experimental setup for optospectrum meter measurement.

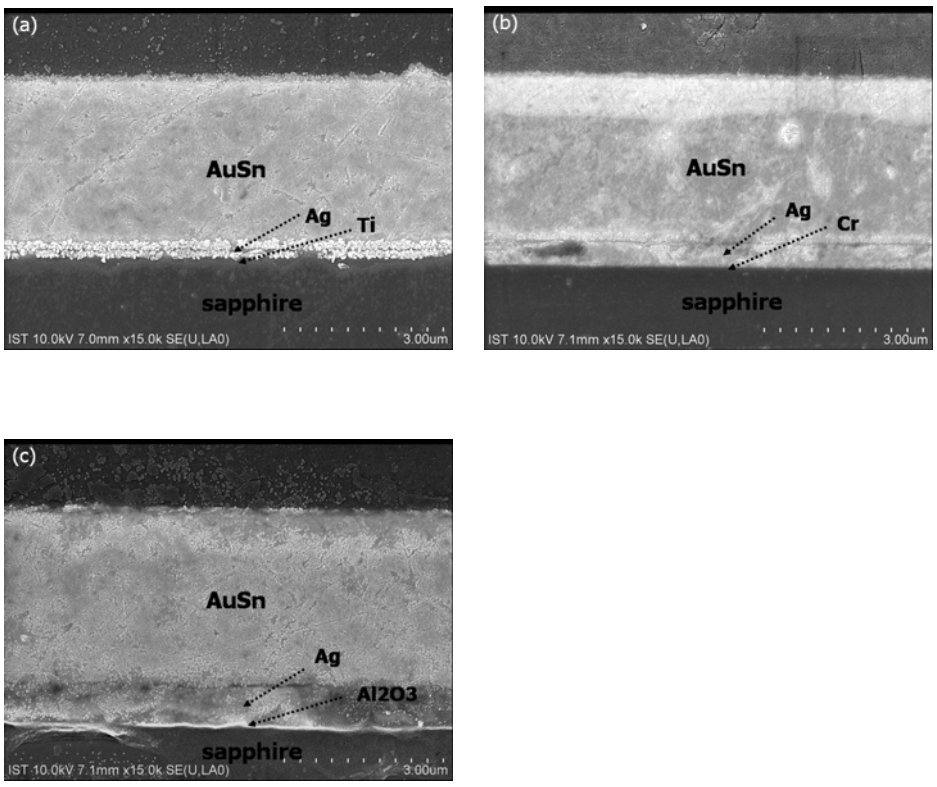

Fig.2. Represented microstructure of the designed reference mirror structures of (a) sapphire/Ti/Ag/AuSn, (b) sapphire /Cr/Ag/AuSn, and (c) sapphire/Al_2O_3/Ag/AuSn structures.

Table 2. Measured reflectance and transmittance values
with various coating materials and coating thickness.

Hitachi U-4100			
Symbol	**Wavelength @ 460 (nm)**	**Reflectance (%)**	**Transmittance (%)**
Cal.	**Calibration using Al mirror**	99.9	---
Cal.	**Calibration in air**	---	99.9
Sub.	**sapphire substrate**	13.1	91.3
	sapphire/Ti 30nm	14.2	21.9
	sapphire/Ti 60nm	22.1	9.4
	sapphire/Cr 30nm	20.7	7.1
	sapphire/Cr 60nm	24.9	1.5
	sapphire/Al2O3 30nm	10.9	86.8
	sapphire/Al2O3 60nm	10.3	87.9
	sapphire/Ag100nm	47	0
	sapphire/Ag500nm	48.1	0
	sapphire/Ag1000nm	51.6	0
	sapphire/AuSn 3000nm	30.1	0
A1	**sapphire/Ti 30nm/Ag 100nm /AuSn 3000nm**	18.9	0
A2	**sapphire/Ti 30nm/Ag 500nm /AuSn 3000nm**	18.8	0
A3	**sapphire/Ti 30nm/Ag 1000nm /AuSn 3000nm**	18.8	0
A4	**sapphire/Ti 60nm/Ag 100nm /AuSn 3000nm**	21	0
A5	**sapphire/Ti 60nm/Ag 500nm/AuSn 3000nm**	21	0
A6	**sapphire/Ti 60nm/Ag 1000nm/AuSn 3000nm**	22.4	0
B1	**sapphire/Cr 30nm/Ag 100nm/ AuSn 3000nm**	26.2	0
B2	**sapphire/Cr 30nm/Ag 500nm/ AuSn 3000nm**	20.3	0
B3	**sapphire/Cr 30nm/Ag 1000nm/ AuSn 3000nm**	23.6	0
B4	**sapphire/Cr 60nm/Ag 100nm/ AuSn 3000nm**	23.7	0
B5	**sapphire/Cr 60nm/Ag 500nm/ AuSn 3000nm**	27.1	0
B6	**sapphire/Cr 60nm/Ag 1000nm/ AuSn 3000nm**	23.6	0
C1	**sapphire/ Al_2O_3 30nm/Ag 100nm/ AuSn 3000nm**	41.5	0
C2	**sapphire/ Al_2O_3 30nm/Ag 500nm/ AuSn 3000nm**	45.3	0
C3	**sapphire/ Al_2O_3 30nm/Ag 1000nm/ AuSn 3000nm**	44.6	0
C4	**sapphire/ Al_2O_3 60nm/Ag 100nm/ AuSn 3000nm**	45.9	0
C5	**sapphire/ Al_2O_3 60nm/Ag 500nm/ AuSn 3000nm**	46.7	0
C6	**sapphire/ Al_2O_3 60nm/Ag 1000nm/ AuSn 3000nm**	48.4	0

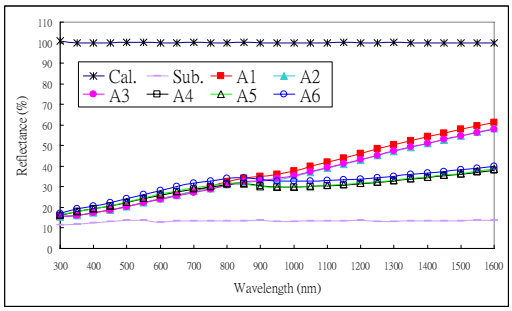

(a)

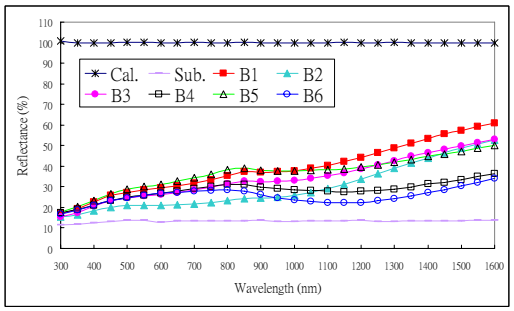

(b)

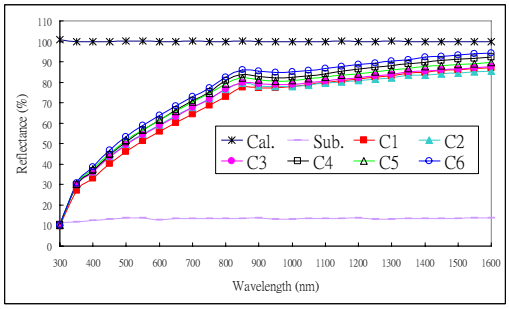

(c)

Fig.3. Reflectance profiles for the (a) sapphire/Ti/Ag/AuSn, (b) sapphire/Cr/Ag/AuSn, and (c) sapphire/ Al_2O_3/Ag/AuSn structures with specimen symbols defined in Table 2.

Hydrous ruthenium oxide coating on Ti and carbon nanotube substrate for the electrode of supercapacitor

H.-S. Hwang[1] and Yuli Lin[1,*]

[1]Institute of Engineering and Science, Chung Hua University,
No.707, Sec.2, Wu-Fu Rd., Hsinchu 300, Taiwan R.O.C.
[*]e-mail: yulilin@chu.edu.tw, TEL:886-3-5186494, FAX: 886-3-5186521

Keywords: Hydrous ruthenium oxide, Carbon nanotube, Supercaoacitor

Abstract. In this study, hydrous ruthenium oxide was deposited on titanium(Ti) and carbon nanotube(CNT) substrate by cathodic deposition method. Combination of amorphous and nanocrystalline structure of hydrous ruthenium oxide was investigated by HRTEM for hydrous ruthenium oxide coating on Ti substrate and CNT substrate. The capacitance was found keeping nearly constant through charge/discharge processes for the coating on Ti substrate during charge/discharge processes. On the other hand, thin and uniform layer of hydrous ruthenium oxide coating can be deposited on CNT substrate. The thickness of the coating layer was found less than 10nm. The consumption of coating was found very effective for the hydrous ruthenium oxide coating on CNT substrate after 10^5 charge and discharge cycles. The capacitance was found decreasing tremedenously through charge/discharge processes for the coating on CNT substrate.

1.Introduction

Nowadays, capacitor has been extensively used for offering the function of equalizing distribution of power. However, the capacitor used today could only provide limited density of power which was not suitable for those electrical appliances needing high-density of power to start. Supercapacitors have many advantages using in electrical devices for their larger electrical capacity, high power density and long cycle life [1]. While, how to manufacture a supercapacitor which is thin, light and elaborate is still a task.

Supercapacitor (Electrochemical Capacitor) is a kind of storage of electricity between secondary battery and capacitor. Comparing with secondary battery, supercapacitor does not only have higher density of power but also can be recharged many times. It also has larger density of energy, offering higher transient power and higher reliability. In general, supercapacitors can be classified into two categories, namely, pseudo-capacitors [2] and double-layer capacitors [3]. The former stores electrical charges in electrode surface by faradic reaction. While, in the latter, electrical charges are stored at the double-layer formed at electrode/electrolyte interface. Various methods have been utilized to manufacture electrode including cyclic voltammetric method [4], sol-gel method [5], cathodic deposition method [6] and etc. Hydrous ruthenium oxides were found to be a superior material for supercapacitor, which can offer higher capacity of electric charge than any other materials. Utilizing hydrous ruthenium oxide ($RuO_2 \cdot xH_2O$) as a supercapacitor material, the H^+ transits easily in itself, and Ru^{4+} could increase the capacity. Ruthenium not only has several different oxide forms; but also could go on oxidation reduction itself [7].

2.Experimental Procedure

In this study, hydrous ruthenium oxide with and without dispersed Carbon Nanotube (CNT) additives was deposited on Ti substrate by cathodic deposition method. Ti substrate was first cleaned thoroughly by acetone and followed by chemical etching of 5%HF for 5 minutes and 50%HCl for 15 minutes. The purpose of acid etching is to increase the adhesion between the coating layer and the Ti substrate. Carbon Nanotube has been dispersed by ultrasonic method to avoid agglomeration during deposition processes. The concentration of CNT added in the deposition process was 0.05 wt%. Two kinds of specimens were prepared in this study, hydrous ruthenium oxide was coated on Ti substrate on one specimen, and hydrous ruthenium oxide was coated on both Ti and CNT substrate on the other specimen. The time of specimens which were immersed into the deposition bath is 60 minutes. The electrical capacity characteristics of specimen were examined by cyclic voltammetry. Because of the hydrous ruthenium oxide is amorphous or nanocrystalline structure, the microstructure of hydrous ruthenium oxide coating is best elucidated by high resolution transmission electron microscopy (HRTEM). In this study, specimens were also tested through charge/discharge cycles for 10^5 times at 1000 mV/s on 0.5M H_2SO_4 to examine the effect on the microstructure as well as the capacitance.

3. Results and Discussion

3.1 Microstructural investigation of hydrous ruthenium oxide coating

Figure 1(a),(b) and 2(a),(b) show the HRTEM images of hydrous ruthenium oxide coating on Ti

substrate before and after charge/discharge processes, respectively. Nanosized particles (about 2 nm) embedded in an amorphous phase can be observed both on specimens before and after charge/discharge processes. It is well known that the content of water molecules per RuO2 on hydrous ruthenium oxide affect the capacitance of coating [8-9]. The results from measured capacitance and EDX suggest that our coating have the approximate formula of $RuO_2 \cdot H_2O$ for coating on Ti substrate both on specimens before and after charge/discharge conditions. Figure 3(a),(b) reveals the nanostructure of hydrous ruthenium oxide coating on CNT substrate before charge/discharge processes. Uniform hydrous ruthenium oxide layer can be coated on CNT substrate. The thickness of the coated layer was found less than 10nm. The hydrous ruthenium oxide layer consists of nanosized particles whose size is about 3-5 nm. Amorphous phase can also be observed on this specimen. Besides, it can be clearly observed in Figure 4(a) and (b) that the thickness of coated layer was found decreasing after charge/discharge processes indicating the consumption of coating was found very effective for the coating on CNT substrate after 10^5 charge /discharge cycles. The results from measured capacitance and EDX demonstrate that our coating have the approximate formula of $RuO_2 \cdot H_2O$ for coating on CNT substrate before charge/discharge processes. However, the structure of hydrous ruthenium oxide on CNT substrate after charge/discharge processes could be changed to anhydrous RuO_2 or hydrous RuO_2 with very few water content.

3.2 Capacitance Characterization during charge/discharge processes

The capacitance of specimen of hydrous ruthenium oxide without adding CNT before

charge/discharge cycle was measured to be 363F/g. The capacitance was decreased to 331F/g after 10^5 charge/discharge cycles indicating more stable characteristics during charge/discharge processes on the specimen without adding CNT. On the other hand, the capacitance of specimen of hydrous ruthenium oxide with adding CNT before charge/discharge cycle was measured to be 681F/g. The capacitance was decreased to 257F/g after 10^5 charge/discharge cycles. Although the measured capacitance can be increased with adding CNT on the deposition processes, it was found that the capacitance was dropped tremendously after charge/discharge processes. The decrease on capacitance could be due to: (a) parts of the hydrous ruthenium coating on CNT substrate were detached from hydrous ruthenium coating on Ti substrate during charge/discharge processes or (b) structure of hydrous ruthenium oxide could be changed to anhydrous RuO_2 or hydrous RuO_2 with very few water content.

4. Summary

1. Nanosized particles embedded in an amorphous phase can be observed both on specimens before and after charge/discharge processes for hydrous ruthenium coating on Ti and CNT substrate.
2. Uniform hydrous ruthenium oxide layer can be coated on CNT substrate. Nanosized particles embedded in an amorphous phase can also be observed both on specimens before and after charge/discharge processes for hydrous ruthenium coating on CNT substrate..
3. The capacitance was found keeping nearly constant through charge/discharge processes for the coating on Ti substrate. On the other hand, the capacitance was found decreasing tremedenously

through charge/discharge processes for the coating on CNT substrate.

5. Acknowledgements

This research was partially supported by NSC96-2221-E-216-013 and CHU96-2221-E216-013.

6. References

1. P.Baker, Power Engineering Society Summer Meeting, 2002 IEEE, 1, 21-25, 316-320 (2002).
2. M. F. Rose and S. A. Merryman, Energy Conversion Engineering Conference, 1996. IECEC 96. Proceedings of the 31st Intersociety, 1, 11-16 , 245 -250 (1996 IEEE).
3. C.Arbizzani, M. Mastragostino, F.soavi, Journal of Power Sources 110, 164-170（2001）.
4. C-C. Hu, Y-H. Huang, Electrochimica Acta 46, 3431-3444（2001）.
5. V. Horvat-Radošević, K. Kvastek, M. Vuković, D. Čukman, Journal of Electrochemical Chemistry 482, 188-201（2000）.
6. Y. Lin, H.-S. Hwang and W-J. Lee, Microscopy and Microanalysis, 13, Supp. 2, 994-995 (2007),
7. B. Park, C.D. Lokhande, H.-S. Park, K.-D. Jung, O.-S. Joo, Journal of Power Source, 134, 148 (2004).
8.W.Dmowski, T.Egami, K.E.Swider-Lyons, C.T. Love and D.R.Rolison, J.Phys.Chem. B, 106, 12677-12683 (2002).
9.D.A.McKeown, P.L.Hagans, L.P.L. Carette and A.E. Russell, J.Phys.Chem. B, 103, 4825-4832 (1999).

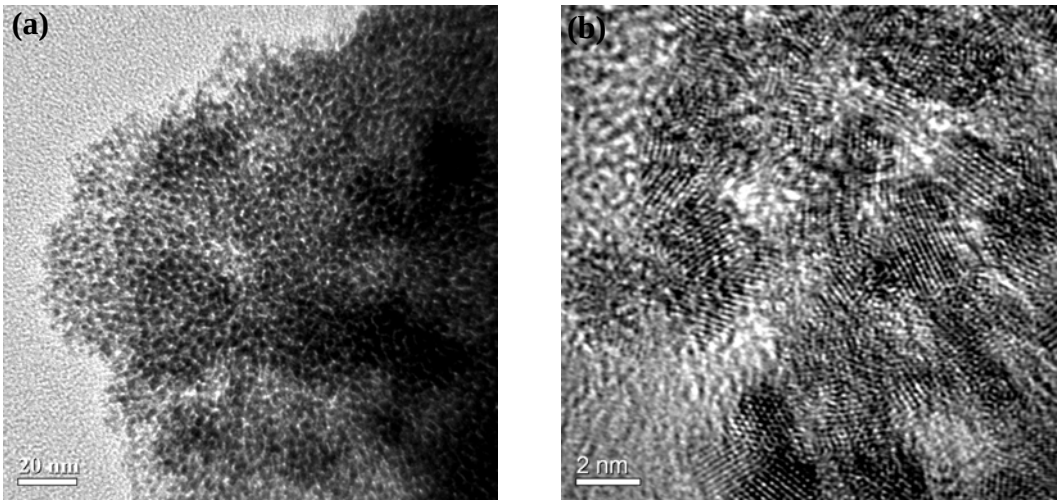

Figure 1. HRTEM images of $RuO_2 \cdot xH_2O$ on Ti substrate before charge/discharge cycles, (a) lower magnification and (b) higher magnification form (a).

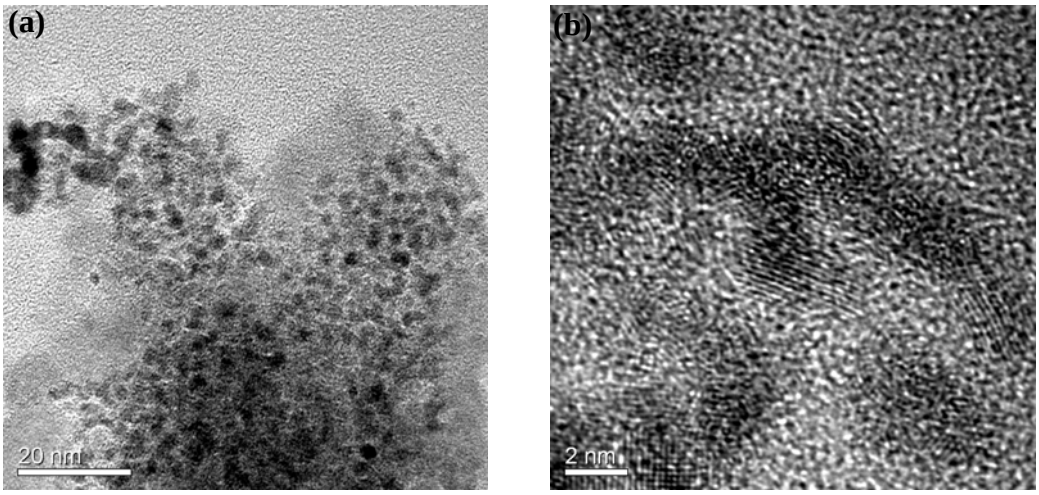

Figure 2. HRTEM images of $RuO_2 \cdot xH_2O$ on Ti substrate after 10^5 cycles of charge/discharge, (a) lower magnification and (b) higher magnification form (a).

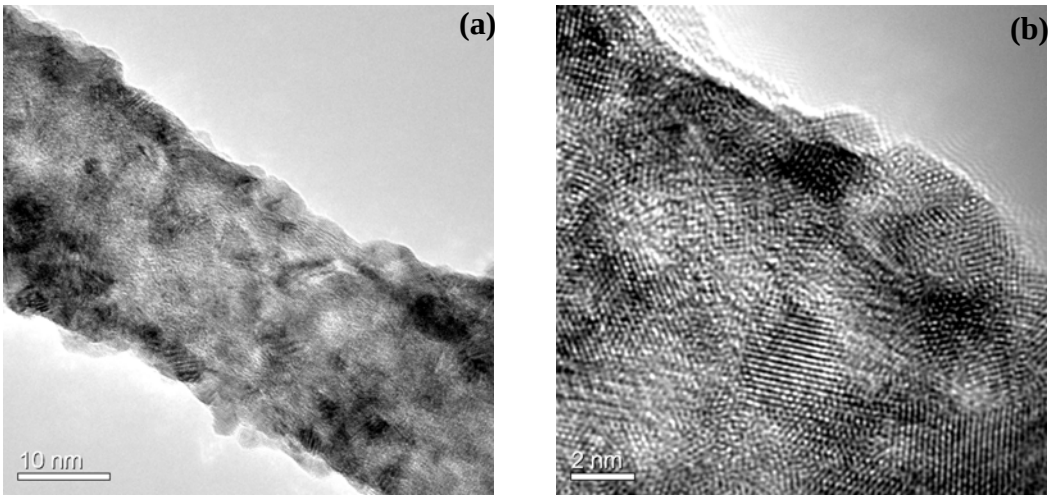

Figure 3. HRTEM images of $RuO_2 \cdot xH_2O$ on CNT subatrate before charge/discharge cycles, (a) lower magnification and (b) higher magnification form (a).

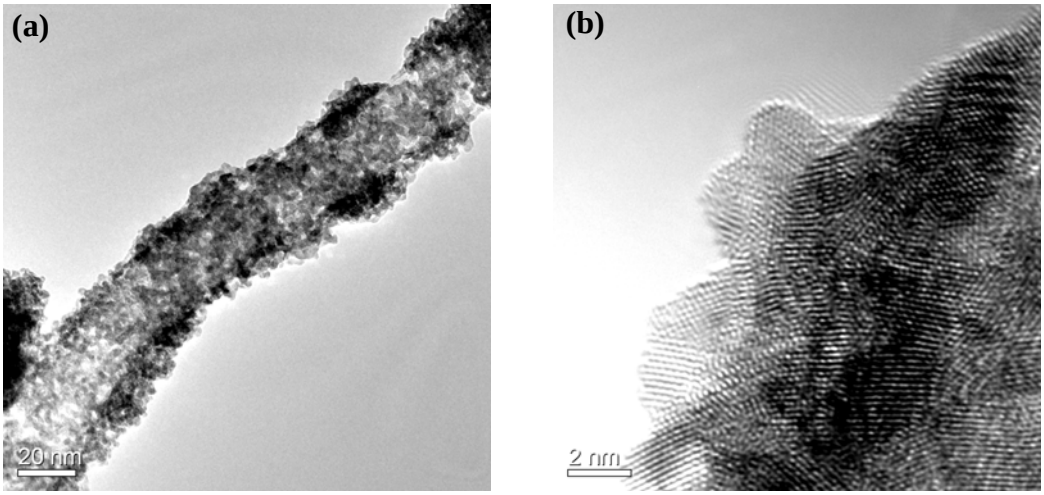

Figure 4. HRTEM images of $RuO_2 \cdot xH_2O$ on CNT subatrate after 10^5 cycles of charge/ discharge, (a) lower magnification and (b) higher magnification form (a).